

Effect of preparation method on activity and stability of LaMnO_3 and LaCoO_3 catalysts for the flameless combustion of methane

E. Campagnoli^a, A. Tavares^b, L. Fabbrini^a, I. Rossetti^a,
Yu.A. Dubitsky^b, A. Zaopo^b, L. Forni^{a,*}

^aDipartimento di Chimica Fisica ed Elettrochimica, Università degli Studi di Milano, Via C Golgi, 19, I-20133 Milano, Italy

^bPirelli Labs SpA, V.le Sarca, 222 Milano, Italy

Received 10 March 2004; received in revised form 27 July 2004; accepted 28 July 2004

Available online 15 September 2004

Abstract

A set of LaMnO_3 and LaCoO_3 catalysts was prepared through different synthesis procedures. The selected techniques included the sol–gel method, flame hydrolysis from aqueous solution, complexation through EDTA and solid-state reaction. The last was accomplished through reactive grinding by ball-milling either in a vibration mill or in a planetary mill. EDTA complexation was applied for LaCoO_3 only and did not improve significantly catalyst activity or stability, with respect to other techniques. Ball-milling never allowed obtaining a pure perovskitic phase, at least under the most energetic grinding conditions permitted by our apparatus. The highest activity for the catalytic flameless combustion of methane was obtained with the sol–gel prepared samples, though thermal resistance revealed insufficient for high temperature applications. A bit lower activity, but coupled with good thermal stability was obtained with the samples prepared through flame hydrolysis. © 2004 Elsevier B.V. All rights reserved.

Keywords: Perovskite-like catalysts; Preparation method; Methane; Catalytic flameless combustion

1. Introduction

The catalytic flameless combustion (CFC) of hydrocarbons is an efficient method for limiting or even virtually suppressing the formation of harmful pollutants during combustion, being carried out at considerably lower temperature (ca. 800 °C). Perovskite-like materials proved to be interesting catalysts for this reaction, being cheaper, comparatively active and much more resistant to deactivation than the traditional noble metal-based catalysts.

Perovskites are mixed oxides of general formula ABO_3 , where both A and B metal ions can be partially substituted, leading to a wide variety of compounds. These are often characterised by oxygen non-stoichiometry, which determines interesting catalytic properties for many reactions [1,2]. Traditionally, these mixed oxides have been prepared

through a calcination-milling (CM) procedure, leading to low surface area, poorly active materials. To overcome this limit, several techniques were developed, among which the so called citrate or tartrate sol–gel (SG) method allows to obtain relatively high surface area, up to two orders of magnitude higher than for the samples prepared by CM [3,4]. Indeed, the formation of the citrate or tartrate complex keeps the cations homogeneously dispersed, allowing obtaining the pure perovskitic phase at low calcination temperature (ca. 500–600 °C). Thus activity of the SG samples is usually high, due to the high surface area. However, these catalysts easily sinter, because of the very low particle size of the powder obtained at so a low temperature. Thermal stability can be made sufficient for CFC application only after calcination at least at 850–900 °C, but this strongly depresses surface area [4].

In some previous papers [5–7] we described a newly developed procedure for the synthesis of perovskites, based on the flame hydrolysis (FH) of an aqueous solution of

* Corresponding author. Tel.: +39 02 50314289; fax: +39 02 50314300.
E-mail address: lucio.forni@unimi.it (L. Forni).

precursor salts. This technique combines the advantages of a relatively high surface area and of the calcination at high temperature, leading to much more stable catalysts.

Some further different preparation techniques can be found in literature. In particular, an EDTA complexation method [8] and a solid-state reaction achieved through ball-milling [9–13]. The ball-milling procedure is reported to be a high energy mechanical synthesis, allowing to attain a pure perovskitic phase at r.t., with surface area as high as 100 m²/g [9,11]. However, once again for high temperature application a pre-calcination step is needed, so depressing surface area by over one order of magnitude after calcination at 700 °C only [10].

The aim of the present work was to compare samples of LaMnO₃ and LaCoO₃ prepared through different procedures. Attention was paid on the effect of preparation method on the main physical–chemical properties of the catalysts and particularly on activity for the CFC of methane and thermal stability, the latter being of fundamental importance in high-temperature application. Finally, the catalyst stability under less oxidising or even reducing conditions was also analysed.

2. Experimental

2.1. Catalyst preparation

2.1.1. Flame-hydrolysis technique

A detailed description of our FH procedure for the preparation of perovskitic samples is given elsewhere [5,7]. Briefly, samples Mn-FH and Co-FH (Tables 1 and 3) were prepared by dissolving stoichiometric amounts of La(CH₃COO)₃·H₂O and Mn(NO₃)₂·4H₂O or Co(NO₃)₂·6H₂O, respectively, in distilled water. Citric acid was then added as complexing agent in molar ratio 0.5/1 with respect to the sum of metal salts. The resulting solution was nebulised into a H₂ + O₂ flame through a small nozzle. The residence time in the hottest zone of the flame, whose estimated temperature was 1600–1800 °C, was ca. 3 ms. The finely powdered product was then collected by means of a 10 kV electrostatic precipitator.

Table 1
Main properties of LaMnO₃ catalysts

Sample	BET SSA (m ² /g)	XRD ^a	T _{1/2} (°C) ^b	T _f (°C) ^b	T _f (°C) ^c	T _f (°C) ^d
Mn-SG	25.5	P	395	453	504	531
Mn-FH	19.3	P	489	605	677	677
Mn-EDTA	n.d. ^e	A	n.d.	n.d.	n.d.	n.d.
Mn-BMP1	n.d.	A	569	>650	n.d.	n.d.
Mn-BMP2	3.0	A	561	>650	n.d.	n.d.

^a P: Perovskite, A: Amorphous.

^b Standard activity test.

^c R1 test.

^d R2 test.

^e n.d.: not determined.

2.1.2. Sol–gel method

Samples Mn-SG and Co-SG (Tables 1 and 3) were prepared by dissolving in distilled water proper amounts of La(NO₃)₃·6H₂O and Mn(NO₃)₂·4H₂O or Co(NO₃)₂·6H₂O and by adding citric acid in 1/1 molar ratio with respect to the sum of metal salts. The solvent was evaporated in vacuo (50 °C, residual pressure 25 Torr) and the viscous product obtained was then dried in vacuo for 9 h (70 °C, residual pressure 35 Torr). Finally, the sample was calcined at 700 °C for 1 h in flowing air.

2.1.3. EDTA method

Samples Mn-EDTA and Co-EDTA (Tables 1 and 3) were prepared as described in [8], by dissolving the proper amount of EDTA in distilled water, so to have a 1/1 molar ratio with respect to the sum of metal salts. After adjusting the pH of the solution to 9 by addition of aqueous NH₄OH, a solution of the precursor salts in proper amounts was added. The resulting solution was neutralised and heated to 80 °C. H₂O₂ was then added. The solid product so obtained was filtered, dried at 100 °C for 4 h and calcined at 700 °C for 1 h.

2.1.4. Ball-milling technique

Some LaMnO₃ samples were prepared by ball-milling a mixture of the precursor oxides (La₂O₃ + Mn₂O₃). The first attempt (samples Mn-BMV, Table 2) was made by means of a vibration mill (Retsch, mod. MM200, with 10 cm³ zirconia jar and two 12 mm zirconia balls). The mixture was milled at 1100 rpm for upto 50 h. Different milling procedures were followed: dry, slurry or after addition of grinding aids. The Mn-BMP samples (Table 2) were prepared by using two planetary mills (Fritsch, Pulverisette 4 and Pulverisette 7, respectively). The milling conditions were 400 and 800 rpm, with 10 and 12 mm zirconia balls for the two models, respectively, and milling time 6 or 24 h.

2.2. Catalyst characterisation

BET specific surface area was determined by N₂ adsorption–desorption, by means of a Micromeritics ASAP 2010 instrument. The crystalline phases were recognised through powder X-ray diffraction (XRD) by means of a Philips PW1820 diffractometer, Cu Kα radiation (λ = 1.5418 Å), Ni filtered, and comparing the patterns obtained with literature data [14]. Particle size was determined by means of a Cambridge Stereoscan 150 scanning electron microscope (SEM).

2.3. Catalytic activity and catalyst deactivation

The activity for the CFC of methane was measured by means of a bench scale continuous apparatus. Standard reaction conditions were as follows: 0.12 cm³ of catalyst, diluted with 1.3 g of quartz, both in 0.15–0.25 mm particle size, were loaded into a tubular quartz reactor (7 mm i.d.),

Table 2
Milling aid for the preparation of LaMnO₃ by ball-milling

Sample	Milling aid	Milling aid solvent	Concentration of added milling aid
Mn-BMV4	Ethyleneglycol	Ethanol	ca. 600 ppm
Mn-BMV5	Propyleneglycol	Isopropanol	ca. 600 ppm
Mn-BMV6	TIPA ^a	Water	ca. 1000 ppm
Mn-BMV8	TIPA	Isopropanol	ca. 1000 ppm
Mn-BMP1	None	–	–
Mn-BMP2	None	–	–

^a TIPA: triisopropanolamine.

heated by an electric furnace, controlled by an Eurotherm 812 TRC. The catalyst was activated in flowing air (20 cm³/min), while increasing temperature (10 °C/min) upto 650 °C, then kept for 1 h. After cooling in flowing air down to 250 °C, the gas flow was switched to a mixture of 10 cm³/min of 1.04 vol% CH₄ in He + 10 cm³/min of air. The gas flow rates were regulated by means of MKS 1259 mass flow-meters, governed by a MKS 247 control unit. The temperature was increased (2 °C/min) upto 650 °C, while monitoring methane conversion by means of an in line HP 5890A TCD gas chromatograph. Two additional tests were also made to check catalyst activity and stability in less oxidising conditions. The gas flow rates were regulated so to obtain O₂/CH₄ = 2.4 mol/mol ratio (test code R1, Table 1) or 1.4 mol/mol ratio (test code R2), values to be compared with the standard test conditions of O₂/CH₄ = 20 mol/mol ratio (test code S).

Thermal stability was checked after the standard activity test by overheating the sample upto 800 °C for 24 h. The temperature was then lowered down to the temperature of maximum conversion (*T_p*, as determined during the standard activity test) and methane conversion was measured once again. Three heating cycles were then performed, during which temperature was raised to 800 °C, kept for 1 h, and lowered back to *T_p*, to check for any change in methane conversion.

2.4. TPD–TPR–QMS analysis

The apparatus and procedure are described elsewhere [7,15]. Briefly, ca. 0.20 g of catalyst were loaded into a continuous, tubular quartz microreactor, fed with 20 cm³/min of superpure He (purity ≥99.9999 vol%) and heated by an electric furnace, controlled by an Eurotherm 2408

TRC. The composition of the outlet gas was analysed by means of a quadrupole mass spectrometer (QMS) (MKS, PPT Residual Gas Analyser). TPD of pre-adsorbed O₂ was carried out in 20 cm³/min flowing He, after overnight saturation in 20 cm³/min flowing air (purity ≥99.9995 vol%) at 750 °C and back to 50 °C, always in flowing air. Prior to desorption the sample was equilibrated in 20 cm³/min flowing He at 50 °C, then heated (10 °C/min) upto 800 °C. A further TPD experiment was carried out to check for the possible adsorption of the substrate. CH₄ pre-adsorption was carried out at different temperatures (50, 100, 200, 500 and 600 °C), by feeding 30 cm³/min of a mixture of 1.04 vol% CH₄ in He for 1 h. The subsequent TPD was carried out following the above-described procedure. Finally, a TPR experiment was carried out by feeding continuously 30 cm³/min of the same CH₄ in He gas mixture through a sample pre-saturated in 20 cm³/min flowing air at 750 °C for 1 h, then heating (10 °C/min) upto 650 °C.

3. Results and discussion

3.1. LaMnO₃ catalysts

3.1.1. Catalyst preparation and characterisation

The sample prepared by the SG method showed the typical XRD reflections of the perovskitic phase [14] only after calcination upto at least 650 °C. A relatively high specific surface area (SSA) was obtained with this preparation procedure (Table 1), together with ca. 0.5 μm particle size. However, when increasing calcination temperature upto 950 °C, a decrease of SSA by ca. one order of magnitude was observed, accompanied by lower catalytic activity (sample Mn-SG, calcined at 950 °C, here not reported). On the other hand, the FH technique [5–7,16], leading to nanometric particles of relatively high SSA (ca. 20 m²/g), calcined at very high temperature (1600–1800 °C), ensured an optimal thermal resistance and high phase purity.

A first attempt to use EDTA as complexing agent was carried out by following the procedure described in [8]. The main difficulty was to achieve the partial oxidation of Mn(II) to Mn(III). According to [8], the oxidation can be made with H₂O₂, which however caused the precipitation of dark-

Table 3
Main properties of LaCoO₃ catalysts

Sample	BET SSA (m ² /g)	XRD ^a	T _{1/2} (°C) ^b	T _f (°C) ^b
Co-SG	12.2	P	390	477
Co-FH	17.9	P	466	602
Co-EDTA (500 °C)	n.d. ^c	A	n.d.	n.d.
Co-EDTA (700 °C)	11.6	P	442	530

^a P: Perovskite, A: Amorphous.

^b Standard activity test.

^c n.d.: not determined.

brown MnO_2 powder. The procedure was then varied by first dropping the $\text{Mn}(\text{NO}_3)_2$ solution into the EDTA one, followed by slowly dropping the H_2O_2 solution, so that no MnO_2 precipitation was observed. After addition of the La precursor, the solvent was removed in rotavapor and the powder obtained was calcined either at 500 or at 700 °C. In both cases the product showed XRD amorphous (Mn-EDTA sample, Table 1).

A further preparation technique was then tested, consisting in solid-state reaction through ball-milling of the precursors oxide mixture, according to [9–13]. The first attempt (sample Mn-BMV1, Table 2) was carried out in the vibration mill under dry conditions and in the absence of any grinding aid [17]. However, the material so obtained was not homogeneous, due to the agglomeration of the powder, preventing any efficient milling of the reagents. The Mn-BMV2 sample was then prepared through ball-milling of a slurry, obtained by suspending the precursor oxide mixture in water. Though the concentration of the suspension was varied, no significant solid-state reaction occurred. Hence, the further attempts were carried out in the presence of some milling aid [18], in very low concentration, even down to a few hundreds ppm. A few drops of a solution of the milling aid in a solvent proved sufficient to prevent powder agglomeration. Details of milling aid addition are given in Table 2. Powder agglomeration during milling is due to the breaking and attrition of the solid particles, which generates electrostatic charges. The milling aid then must prevent the electrostatic interaction between the particles [18]. XRD analysis of the Mn-BMV5 sample after milling for 9, 15, 24 and 35 h showed that after 9 h the perovskitic phase started to be observed, though not predominant. By increasing the milling time the reaction proceeded, but never beyond a given plateau. For example, milling the sample Mn-BMV4 for more than 44 h did not bring any further composition change (Fig. 1). The most efficient milling aid showed tri-isopropanolamine (TIPA). Only one drop of a 25 wt.% aqueous solution of this substance was sufficient to obtain a perfectly flowable and grindable powder (sample Mn-BMV6). However, the conversion to perovskite never went to completeness with any of the milling aids tested, the

XRD reflections of the precursors oxides remaining still present at the plateau level even after milling for over 44 hours. By combining the positive effect of iso-propanol and of TIPA, a last attempt (Mn-BMV8) was carried out using a few drops of a 25 wt.% solution of TIPA in iso-propanol. This gave indeed the best result, the reaction attaining the plateau after 28 h, with ca. 50% conversion to perovskite.

The conclusion that can be drawn is that the mechanical energy provided by the available vibration ball-mill was not sufficient for a complete transformation of the oxide mixture into the perovskitic LaMnO_3 catalysts.

A different apparatus was then tested, i.e. a planetary ball-mill. With this apparatus after 6 h and in the absence of any milling aid, only a partial transformation of the precursors oxides was observed. However, after 24 h the XRD reflections of the parent oxides completely disappeared and an almost amorphous phase was obtained, probably of perovskitic structure, though hardly identifiable by XRD.

3.1.2. Catalytic activity

The specific activity referred to the unit surface area of the catalyst, of the samples Mn-SG and Mn-FH, measured under standard reaction conditions (vide supra) for the CFC of methane, is reported in Fig. 2. The values of $T_{1/2}$ and T_f , representing the temperature of half transformation and of complete CH_4 conversion, respectively, are given in Table 1. As expected, the Mn-FH sample showed values of $T_{1/2}$ and T_f much higher than those of Mn-SG. Indeed, the specific activity referred to unit weight of catalyst, was comparable to that of the Mn-SG sample, but the SSA of the former was rather lower (Table 1). However, the different activity of the SG and FH samples cannot be ascribed to the relatively small difference in surface area only. Indeed, undoped ABO_3 perovskites possess relatively reduced lattice oxygen mobility, partially inhibiting the intra-facial catalytic activity [6,7,19]. Indeed, the activity of perovskites has been ascribed to several parameters, such as ionic conductivity, lattice oxygen mobility [20], reducibility and oxygen sorption properties [21]. In particular, the

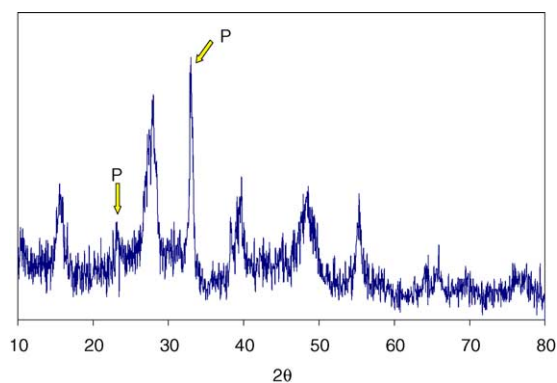


Fig. 1. XRD pattern of the sample Mn-BMV4 after milling for 44 h. P: perovskite main reflections.

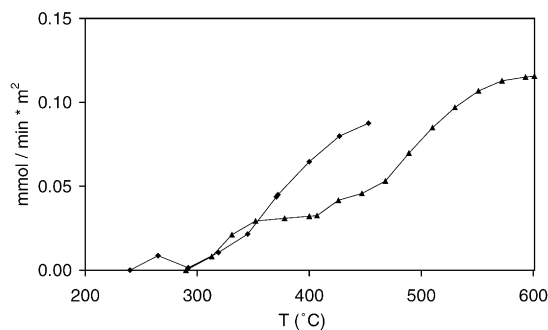


Fig. 2. Specific activity, referred to unit surface area and measured under standard reaction conditions (see text), of samples Mn-SG (◆) and Mn-FH (▲) for the CFC of methane.

mobility of O^{2-} ions determines the mechanism of the oxidation reaction. With undoped samples, the low-temperature supra-facial reactivity can be important [7] and a high surface area leads to a higher concentration of surface sites, active for oxygen adsorption. On this basis a low surface area can be very unfavourable. However, activity through the intra-facial mechanism is mainly due to the presence of lattice defects, whose concentration depends on temperature and duration of the calcination step during preparation. The FH technique adopts very short residence time in a high temperature flame and since defects concentration depend on the calcination temperature more than on its duration, one has to expect a lower concentration of defects in the FH than in the SG sample, influencing the intra-facial activity [22].

To check the activity and stability of the samples under less oxidising or even under reducing conditions, two additional activity tests (R1 and R2, vide supra) have been performed. A strong decrease of conductivity is reported for $LaMnO_3$ treated under reducing conditions, reversible upon oxidation [23]. In fact, at low oxygen partial pressure, the reduction of Mn(III) to Mn(II) can be observed, with destruction of the perovskitic phase [24]. The results of the R1 and R2 tests for the samples Mn-SG and Mn-FH are summarised in Table 1. For both samples less oxidising conditions are penalising, as shown by the increase of T_r . For the Mn-FH catalyst slightly over-stoichiometric or under-stoichiometric conditions led to a similar, strong decrease of activity, while for the Mn-SG sample the activity decrease was less marked and more gradual with decreasing oxygen content in the reacting gas. An explanation of this behaviour can be found in phase stability under reducing conditions [23,24]. XRD analysis after both the R1 and R2 activity tests showed neither destruction of the perovskitic phase, nor XRD-detectable new phase(s) upon reaction under reducing atmosphere. A slight decrease of the BET surface area was observed for the Mn-SG sample only, due to its lower thermal stability (vide infra).

The catalytic activity for the complete oxidation of hydrocarbons on perovskites is connected with lattice oxygen mobility and with the reducibility of the B ion. On this basis the TPD of pre-adsorbed oxygen can be a powerful method for characterising these materials. Heating a perovskite at high temperature in inert atmosphere leads to the formation of oxygen vacancies [25], filled up by a subsequent cooling in air. Charge compensation is provided by partial oxidation of the metal B ion. TPD can reveal two desorption peaks, usually referred to as α and β , appearing in different temperature ranges [1,6]. The low-temperature α -peak is connected with oxygen adsorbed on the catalyst surface and it depends on the concentration of filled oxygen vacancies. The high-temperature β -peak tightly depends on the nature of the B ion, being correlated to its partial reduction to a lower oxidation state [25–27]. The presence of the β -peak and the value of its onset temperature can then be used as a qualitative description of B ion reducibility and

lattice oxygen mobility and both these parameters have a marked effect on catalytic activity.

The intra-facial mechanism involves a redox cycle of metal B ion through the gaseous oxygen present in the reaction atmosphere [28]. A higher reducibility of the B metal, i.e. a low-temperature β -peak, would make easier this step and favour a quicker oxygen transport through the lattice. Undoped $LaBO_3$ catalysts showed extremely low oxygen mobility [7], ionic conductivity increasing with La substitution. However, conductivity is also connected with the reducibility of metal B. Indeed, the activation energy for oxygen transport is reported to be higher for Mn- than for Co-based perovskites [7,20]. In the present work, a slightly lower onset temperature (ca. 550 °C) of the β -peak was observed for the Mn-SG sample, with respect to that reported for the Mn-FH sample (ca. 600 °C) [7]. The same temperature shift was observed for the peak maxima (ca. 650 °C for Mn-SG and 700–750 °C for Mn-FH), confirming the tight correlation between ionic conductivity, B metal reducibility and catalytic activity, the SG sample being more active and reducible than the FH sample.

The additional TPD experiments, carried out after conditioning non-activated samples in flowing CH_4 at different temperatures, ranging between 50 and 600 °C (vide supra), showed in any case no significant methane adsorption, confirming that the reaction mechanism does not involve substrate adsorption and activation [7]. A final TPR test (Fig. 3), carried out by feeding methane on the Mn-SG sample pre-treated in air at 700 °C for 1 h, showed methane consumption accompanied by CO_2 and H_2O formation at temperatures considerably higher than those of the standard activity tests. This confirms that, in the absence of O_2 in the reaction atmosphere, reactivity is shifted towards the onset temperature of the β -peak.

Finally, samples Mn-BMP1 and Mn-BMP2, tested under standard reaction conditions, showed much less active than the catalysts prepared by the other techniques, hardly reaching 80% CH_4 conversion at 600 °C (Fig. 4). This confirms that a good catalytic activity for the CFC of hydrocarbons is tightly connected with the presence of a fully crystalline perovskitic phase.

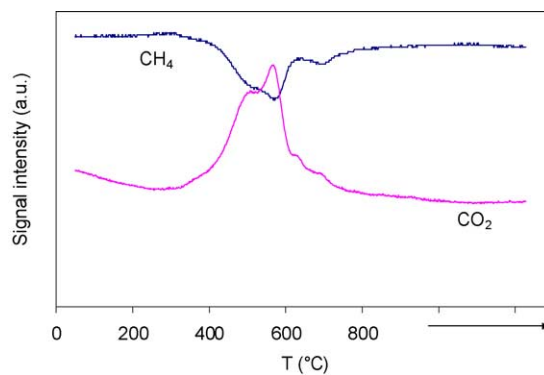


Fig. 3. TPR-QMS pattern in flowing CH_4 , Mn-SG sample, pre-treated 1 h in air at 700 °C.

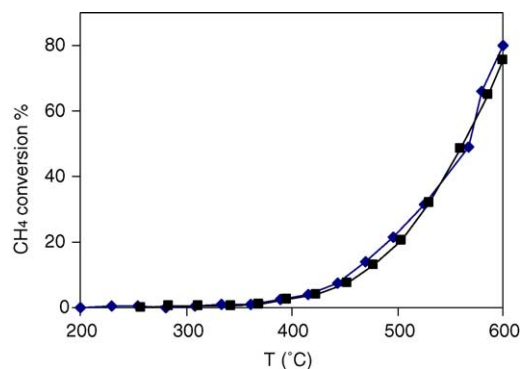


Fig. 4. Catalytic activity for the CFC of methane, referred to unit weight of samples Mn-BMP1 (◆) and Mn-BMP2 (■).

3.1.3. Thermal stability

The results of high temperature deactivation cycles, carried out on both the Mn-SG and Mn-FH samples, are reported in Fig. 5. One may see that thermal resistance of the SG sample was clearly lower than that of the FH catalyst. Indeed, after 24 h on-stream the activity of the FH sample remained unaltered at 100%, while with the Mn-SG sample the conversion dropped to 96%. Moreover, after the initial loss of activity, likely due to a local settlement phenomenon during the first accelerated deactivation cycle, methane conversion over Mn-FH stabilised to ca. 86%. By contrast, the catalytic activity of the Mn-SG sample continued to decrease after every high temperature treatment.

From all the present data it can be concluded that, though the SG procedure allows obtaining initially more active LaMnO_3 catalysts, with respect to the FH technique, the thermal stability of the samples prepared by the former technique is insufficient to sustain high temperature processes, such as the CFC of methane.

3.2. LaCoO_3 catalysts

3.2.1. Catalyst preparation and characterisation

The main physical–chemical properties of these catalysts are reported in Table 3. The comparison between the Co-FH

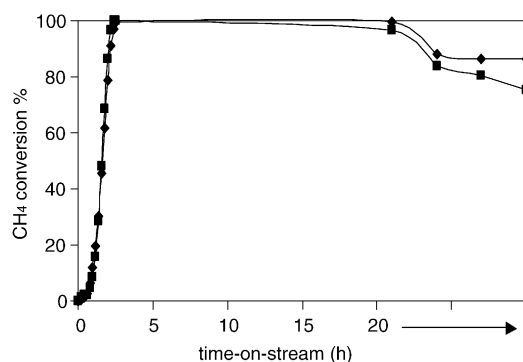


Fig. 5. Thermal stability of samples Mn-SG (■) and Mn-FH (◆). The last three points of each curve refer to the accelerated deactivation cycles at 800 °C.

and Co-SG samples brought to conclusions very similar to those drawn for the La–Mn-based samples. The FH catalyst showed high phase purity, good crystallinity and 20–60 nm particle size. The SG sample, calcined at 650 °C, showed good crystallinity, bigger particles and a lower SSA value with respect to the FH sample.

In spite of the inefficiency of the EDTA procedure for the preparation of the manganites, the method was applied to cobaltite, due to the easier oxidisability of Co(II) to Co(III). The preparation was less complicated than for Mn-EDTA. The precursors solution was first added to the EDTA one. H_2O_2 was then dropped into the resulting solution, leading to an evident colour change from light pink to dark purple, indicating Co(II) oxidation to Co(III). After solvent evaporation the powder obtained was calcined at 500 °C, resulting in a XRD amorphous product. The powder was then calcined at 700 °C, obtaining a pure perovskitic phase, though not fully crystalline, with surface area comparable to that obtained with the SG method.

3.2.2. Catalytic activity

Likewise to manganites, undoped SG samples showed more active than FH samples. In a previous investigation [7] we correlated the catalytic performance of undoped LaBO_3 samples prepared by FH with their TPD patterns of pre-adsorbed oxygen. The presence of supra-facial or intra-facial reaction mechanism was found to be tightly connected with oxygen mobility and with the concentration of oxygen vacancies. Hence, the catalysts with low vacancies concentration (LaFeO_3 and LaMnO_3) revealed more active at low temperature through the supra-facial mechanism and did not show any α -peak in the oxygen TPD pattern. On the other hand, the catalysts showing a more or less intense α -peak (La_2NiO_4 and, to a lower extent, LaCoO_3) were predominantly or exclusively active through the intra-facial mechanism. In line with this, the role of SSA for the present cobaltites seems to be less critical, activity being mainly due to oxygen mobility within the perovskite lattice. Furthermore, the standard activity test carried out with the Co-EDTA (700 °C) sample showed an intermediate activity with respect to Co-SG and Co-FH samples (Table 3). Though the EDTA sample showed a bit more stable (but less active) than the SG sample, and slightly more active, but much less stable than the FH sample, this preparation procedure seems not to add any significant improvement with respect to the SG or FH techniques.

4. Conclusions

From the present results it can be concluded that: (i) No complete oxide conversion was achieved through a vibration ball-milling procedure and no clearly crystalline perovskitic phase was obtained through the planetary ball-milling procedure by means of the available apparatus; (ii) the best results obtained with the vibration ball-milling was 50%

conversion of the precursor oxides to perovskite after 28 h, by using triisopropanolamine dissolved in iso-propanol as grinding aid; (iii) the activity of the samples prepared through ball-milling was lower than that obtained with other preparation procedures; (iv) the EDTA complexation method proved useful for the preparation of LaCoO_3 only. A catalyst less active than the SG sample was obtained, though a bit more stable; (v) the SG method led to more active samples, which however proved insufficiently resistant for a high temperature application; (vi) the FH technique proved the only technique able to provide a sample with good catalytic activity, coupled with the best thermal stability for the CFC of methane.

Acknowledgements

We are indebted to Pirelli Labs SpA for financial aid and for the permission to publish the present data.

References

- [1] N. Yamazoe, Y. Teraoka, *Catal. Today* 8 (1990) 175.
- [2] M.A. Peña, J.L.G. Fierro, *Chem. Rev.* 101 (2001) 1981.
- [3] H.M. Zhang, Y. Teraoka, N. Yamazoe, *Chem. Lett.* (1987) 665.
- [4] H. Arai, T. Yamada, K. Eguchi, T. Seiyama, *Appl. Catal.* 26 (1986) 265.
- [5] R.A.M. Giacomuzzi, M. Portinari, I. Rossetti, L. Forni, *Stud. Surf. Sci. Catal.* 130A (2000) 197.
- [6] R. Leanza, I. Rossetti, L. Fabbrini, C. Oliva, L. Forni, *Appl. Catal. B: Environ.* 28 (2000) 55.
- [7] I. Rossetti, L. Forni, *Appl. Catal. B: Environ.* 33 (2001) 345.
- [8] J. Liu, Z.-Y. Wen, Z. Gu, M.W.Z. Lin, *J. Electr. Soc.* 149 (11) (2002) A1405–A1408.
- [9] V. Szabo, M. Bassir, A. Van Neste, S. Kaliaguine, *Appl. Catal. B: Environ.* 37 (2002) 175.
- [10] V. Szabo, M. Bassir, A. Van Neste, S. Kaliaguine, *Appl. Catal. B: Environ.* 43 (2003) 81.
- [11] US Patent No. 6,017,504 (2000), to Université Laval, Canada.
- [12] A. Trovarelli, F. Zamar, J. Llorca, C. de Leitenburg, G. Dolcetti, J.T. Kiss, *J. Catal.* 169 (1997) 490.
- [13] T. Hibino, K. Suzuki, K.I. Ushiki, Y. Kuwahara, M. Mizuno, *Appl. Catal. A: Gen.* 145 (1996) 297.
- [14] Selected Powder Diffraction Data, Miner. DBM, JCPDS, Swarthmore, PA, 1974–1992, Vol. 1–40.
- [15] L. Forni, M. Toscano, P. Pollesel, *J. Catal.* 130 (1991) 392.
- [16] L. Fabbrini, I. Rossetti, L. Forni, *Appl. Catal. B: Environ.* 44 (2) (2003) 107.
- [17] S. Kaliaguine, A. Van Neste, V. Szabo, J.E. Gallot, M. Bassir, R. Muzychuk, *Appl. Catal. A: Gen.* 209 (2001) 345.
- [18] D. Padovani, A. Bravo, *Chim. Ind. Milan* 84 (2002) 59.
- [19] D. Ferri, L. Forni, *Appl. Catal. B: Environ.* 16 (1998) 119.
- [20] M.S. Islam, M. Cherry, C.R.A. Catlow, *J. Solid State Chem.* 124 (1996) 230.
- [21] J.L.G. Fierro, J.M.D. Tascón, L.G. Tejuca, *J. Catal.* 93 (1985) 83.
- [22] C. Oliva, L. Forni, *Catal. Commun.* 1 (2000) 5.
- [23] J.H. Kuo, H.U. Anderson, D.M. Sparlin, *J. Solid State Chem.* 87 (1990) 55.
- [24] T. Nakamura, G. Petzow, L.J. Gauckler, *Mater. Res. Bull.* 14 (1979) 649.
- [25] H.M. Zhang, Y. Shimizu, Y. Teraoka, N. Miura, N. Yamazoe, *J. Catal.* 121 (1990) 432.
- [26] Y. Teraoka, H.M. Zhang, N. Yamazoe, *Chem. Lett.* (1985) 1367.
- [27] Y. Teraoka, M. Yoshimazu, N. Yamazoe, T. Seiyama, *Chem. Lett.* (1984) 893.
- [28] R.J.H. Voorhoeve, J.P. Remeika, D.W. Johnson, *Science* 180 (1973) 62.